Point-of-Care Testing

International Edition: DOI: 10.1002/anie.201810917
German Edition: DOI: 10.1002/ange.201810917

Rapid, Quantitative, and Ultrasensitive Point-of-Care Testing: A Portable SERS Reader for Lateral Flow Assays in Clinical Chemistry

*Vi Tran, Bernd Walkenfort, Matthias König, Mohammad Salehi, and Sebastian Schlücker**

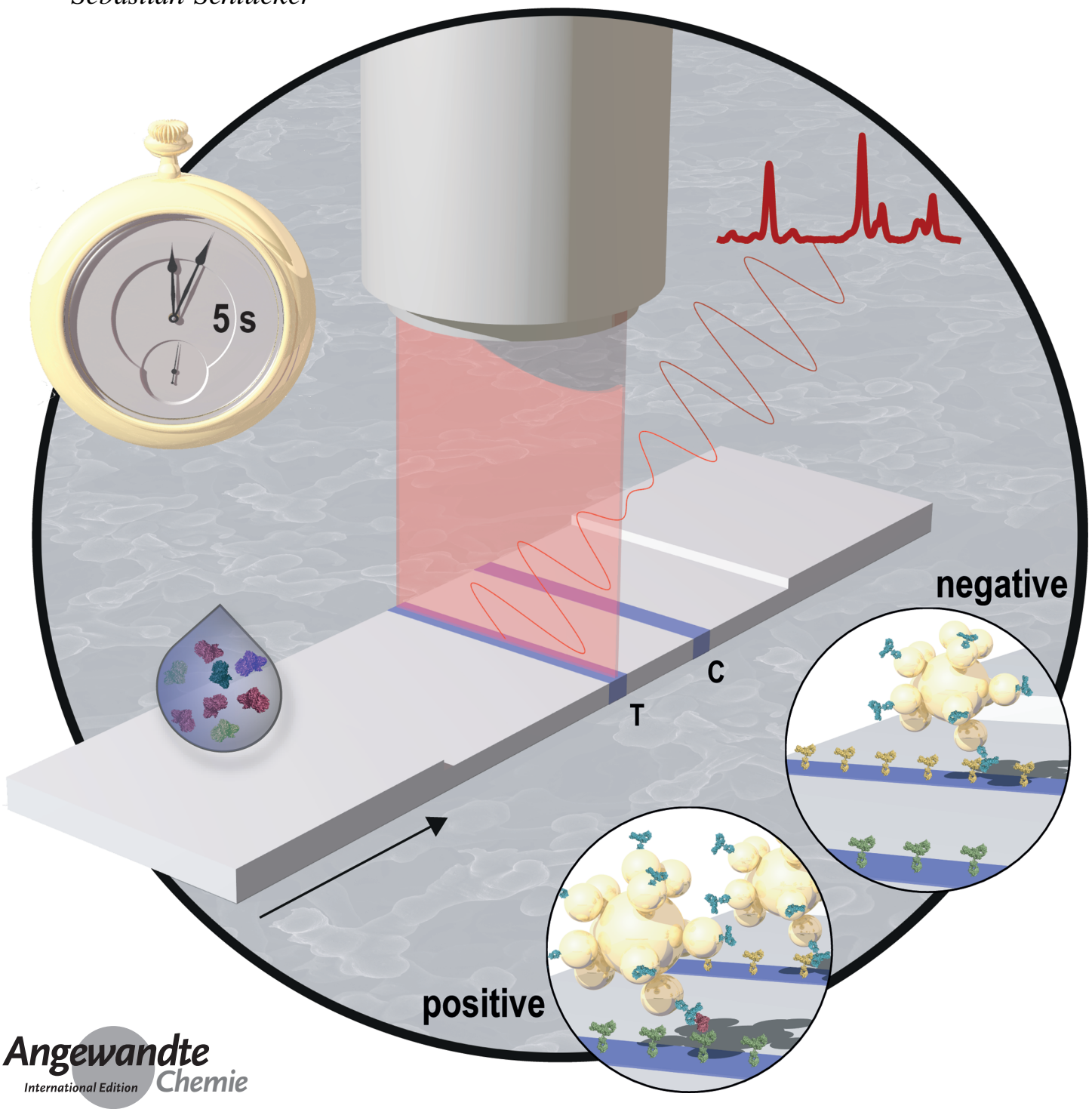

Abstract: *The design of a portable Raman/SERS-LFA reader with line illumination using a custom-made fiber optic probe for rapid, quantitative, and ultrasensitive point-of-care testing (POCT) is presented. The pregnancy hormone human chorionic gonadotropin (hCG) is detectable in clinical samples within only 2–5 s down to approximately 1.6 mIU mL^{-1}. This acquisition time is several orders of magnitude shorter than those of existing approaches requiring expensive Raman instrumentation, and the method is 15-times more sensitive than a commercially available lateral flow assay (LFA) as the gold standard. The SERS-LFA technology paves the way for affordable, quantitative, and ultrasensitive POCT with multiplexing potential in real-world applications, ranging from clinical chemistry to food and environmental analysis as well as drug and biowarfare agent testing.*

Lateral flow immunoassays (LFAs or LFIAs) are widely used portable strips for point-of-care testing (POCT). They are inexpensive and suitable for fast (ca. 10–20 min) and selective detection of target analytes by the naked eye, typically using gold-nanoparticle-labeled antibodies with their characteristic reddish color. The LFA technology is user-friendly and easy to perform anytime and anywhere. The most prominent example is the pregnancy test. The outcome of the test is based on the appearance of a colored line, the so-called test line (TL), which indicates the presence of the target analyte. In contrast, the control line (CL) of the test must always be visible, irrespective of whether the target analyte is present or not; otherwise, the test is invalid. For semiquantitative measurements the color density can be determined by a reader. Nevertheless, this type of optical readout is limited by low sensitivity and precision.[1] The detection of multiple analytes (multiplexing) on the same TL is also not possible as the reader cannot distinguish between gold nanoparticles conjugated to a set of antibodies directed against the different targets.

LFA in combination with surface-enhanced Raman scattering (SERS)[2] is a new and highly promising technology platform, already reported in the pioneering work of Choo and co-workers as well as by Blanco-López, Graham, and co-workers.[3] SERS-based LFAs using antibodies conjugated to molecularly functionalized plasmonic nanoparticles (NPs) with narrow Raman fingerprints[4] can overcome the above-mentioned problems faced in conventional LFAs as they combine high sensitivity, quantification, and multiplexing.[3,5]

The major drawback of current SERS-based LFAs is the readout time until the test result is available for the user. This technical problem arises from the large areas (TL: typically 3–7 mm width × 1–2 mm length), which are typically raster-scanned by (confocal) Raman microscopy with micrometer-sized laser spots and hundreds to thousands of pixels. At each pixel the Raman/SERS spectrum is recorded with integration times of typically 0.1 s to several seconds before the *xy* stage of the microscope moves to the next position. Overall, this acquisition of Raman spectra over hundreds to thousands of pixels results in total acquisition times of dozens of minutes to several hours. This is of course unacceptable for users of POCT in real-world applications.

We have therefore designed and built a portable SERS reader for rapid scanning of the test strip (Figure 1). Line illumination[6] along the entire width of the TL (4 mm) is achieved by a custom-designed fiber optical probe with a line focus (b) in combination with a powerful yet compact 785 nm diode laser (c). Averaging over the entire area of the TL is achieved by scanning the test strip orthogonal to the line focus using a motorized stage. Specifically, we scanned over 50 positions, starting from shortly before to shortly after the TL, with 100 ms per step; this results in an overall acquisition time of only 5 s (see Figure 1a, enlarged image top right). This rapid detection is several orders of magnitude faster than conventional Raman point mapping acquisition schemes. Our reader makes the SERS-LFA technology both feasible (fast and easy-to-use) and affordable (compact reader vs. expensive confocal Raman microscopes) for end users of Raman-based POCT outside academic laboratories.

Au/Au core/satellite nanoparticles comprising an approximately 50 nm large spherical core and about 17 nm small citrate-stabilized satellites were synthesized by electrostatic assembly between the positively charged core and the

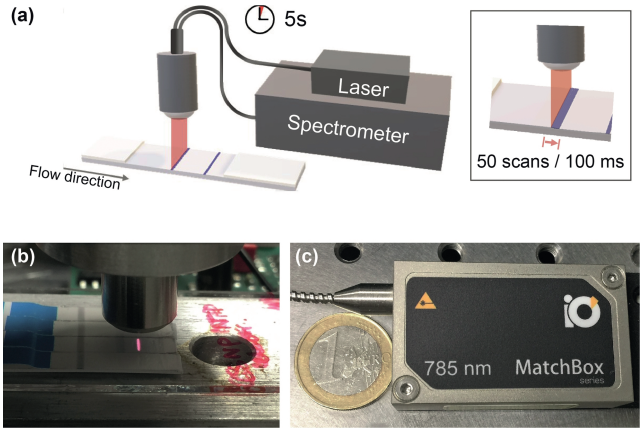

Figure 1. Portable Raman/SERS reader with a custom-designed optical fiber probe with laser line focus: a) Schematic representation of the setup: An averaged Raman spectrum from the entire TL (ca. 4 mm) is obtained within only 5 s by illuminating along the entire width of the TL with a line focus and then moving the test strip orthogonally to it using a motorized stage. b) Photograph of the custom-designed optical fiber probe. c) Photograph of the powerful (up to 450 mW) yet compact 785 nm diode laser.

[*] V. Tran, B. Walkenfort, Dr. M. König, Dr. M. Salehi, Prof. S. Schlücker
Department of Chemistry
Center for Nanointegration Duisburg-Essen (CENIDE)
and Center of Medical Biotechnology (ZMB)
University of Duisburg-Essen
Universitätsstraße 5, 45141 Essen (Germany)
E-mail: sebastian.schluecker@uni-due.de
Supporting information and the ORCID identification number(s) for the author(s) of this article can be found under: https://doi.org/10.1002/anie.201810917.

negatively charged satellites. The core was functionalized with the Raman reporter molecule thio-2-napthol (TN) and the linker molecule (11-mercaptoundecyl)-*N*,*N*,*N*-trimethylammonium bromide (MUTAB). Plasmonic coupling between core and satellites provides the necessary high local field enhancements ("hot spots")[7] for the Raman reporter molecules in the multiple narrow gaps between core and satellites. The anti-hCG detection antibody (Ab) was conjugated to the SERS nanotags via electrostatic attraction. Free binding sites on the nanotags were blocked using phosphate buffered saline (PBS) buffer with 1% bovine serum albumin (BSA). After washing several times with buffer solution, the SERS-labeled detection antibody was ready to use in the LFA.

For a direct and fair comparison with conventional LFAs as the current gold standard, we employed the SERS-labeled detection Ab in combination with a commercially available human chorionic gonadotropin (hCG) pregnancy test. The test comprises a sample pad, a conjugate pad, a nitrocellulose (NC) membrane, and an absorbent pad (Scheme 1, top right). For the SERS-based LFA, the conjugate pads containing the immobilized conventional AuNP conjugates were removed from the commercially available test strips. The SERS-labeled detection Ab was mixed with clinical samples containing a known hCG level and then dropped onto the sample pad of the hCG test (Scheme 1, top left). Upon recognition of the target hormone hCG, the corresponding antigen/Ab complex is formed and flows through the NC membrane in a process driven by capillary forces. The capture Ab required for the formation of the sandwich complex (capture Ab/hCG antigen/detection Ab) is present at the TL. In a positive test (Scheme 1, left), that is, in the presence of the hCG antigen, the sandwich complex can form, and the test line becomes colored. In contrast, in a negative test (Scheme 1, right), that is, in the absence of the hCG antigen, the sandwich complex cannot form, and the test line remains uncolored. In both cases, the CL becomes colored as the corresponding immobilized control Ab directly recognizes the detection Ab (no antigen required).

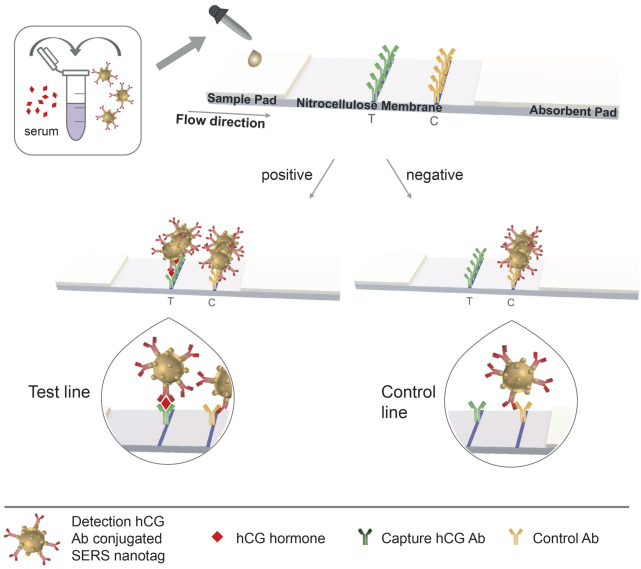

Scheme 1. The SERS-labeled anti-hCG detection antibodies were mixed with clinical serum samples. The corresponding sandwich complex with the capture Ab can only form at the test line in the presence of the pregnancy hormone hCG (left: positive test).

The CL therefore indicates the functionality of the entire LFA. Diluted clinical samples with hCG analyte concentrations ranging from 1678.9 mIU mL^{-1} to 0.8 mIU mL^{-1} were investigated. In addition, a negative control without hCG analyte was carried out to investigate the extent of non-specific binding of the SERS-labeled anti-hCG detection Ab to the NC membrane and to the test line. Every SERS readout at the test line with the portable SERS reader (50 steps, 100 ms each) was repeated five times. A baseline correction was applied to the Raman spectra, and the integrated Raman intensity of one of the dominant peaks of the reporter molecule thio-2-naphthol around 1064 cm^{-1} was determined.

TN, MUTAB, and BSA were purchased from Sigma–Aldrich. Monoclonal mouse anti-hCG detection Ab was obtained from antikoerper-online. The pregnancy hCG test for human serum and urine (gabmed GmbH) was purchased in a local pharmacy store. The manufacturer's LOD is 25 mIU mL^{-1} hCG. The clinical sample, received from Klinikum Osnabrück, with a known hCG concentration is a mixture of sera from ten pregnant women (pooled human serum) in accordance with national ethical guidelines.

The SERS nanotags were characterized by UV/Vis extinction spectroscopy (JASCO V-630 spectrophotometer), dynamic light scattering (DLS, Wyatt Möbius), transmission electron microscopy (TEM, Zeiss EM 910, 120 kV), and scanning electron microscopy (SEM, Jeol JSM 7500F, <5 kV). A home-built optical setup with 660 nm diode laser excitation was employed for simultaneous recording of both elastic and inelastic scattering from single SERS nanotags in real time in suspension.[8] A home-built portable SERS reader comprising a compact 785 nm diode laser (Integrated Optics, laser output: 120 mW), a custom-designed fiber optical probe for line illumination (Inphotonics; width of line focus ca. 4 mm, covering the whole width of the TL), and a compact spectrometer (Ocean Optics QE Pro) were used for the SERS-LFA. The presence of the SERS nanotags on the NC membrane of the LFA strip was additionally confirmed by SEM (Zeiss FIB-SEM 540 Crossbeam, 5 kV).

Highly sensitive SERS-LFAs require very bright SERS nanotags for bioconjugation to the corresponding antibody in order to detect very low amounts of the target analyte. We decided to employ Au/Au core/satellite particles with short gap distances (ca. 2 nm) between the satellites and the core for strong plasmonic coupling and thereby large field enhancements for generating strong SERS signals from the Raman reporter thio-2-naphthol (TN).[7]

The EM images of a single approximately 85 nm large Au/Au core/satellite particle in Figure 2a show that the satellites were relatively evenly distributed over the surface of the core. Correlative Rayleigh/SERS single particle (SP) imaging[8] demonstrates that the majority of the Au/Au core/satellite particles is SERS-active at the SP level (Figure 2b), which clearly demonstrates the high SERS brightness of the nanotags. UV/Vis extinction spectra and dynamic light scattering (DLS) data are given in the Supporting Information, Figure S1. The high reproducibility of the synthesis of the core/

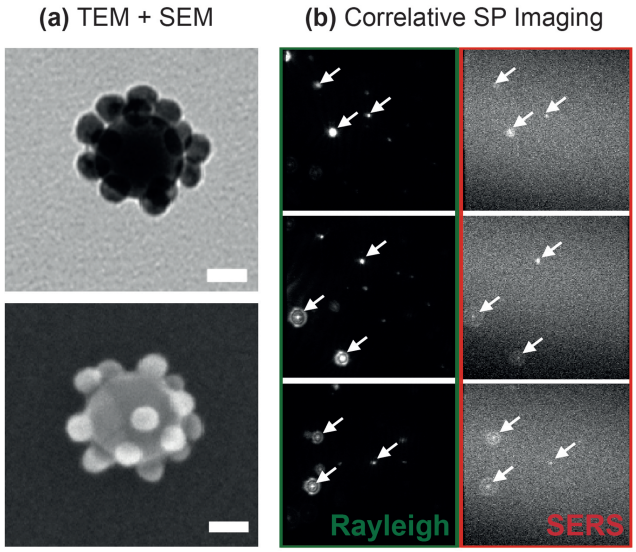

Figure 2. Characterization of the Au/Au 50 nm core/17 nm satellites at the single-particle level. a) TEM image (top, scale bar: 25 nm) and SEM image (bottom, scale bar: 20 nm). b) SERS activity monitored in real time using a home-built optical setup for simultaneous correlative Rayleigh and Raman imaging in suspension[8] (λ_{ex} = 660 nm, laser power = 100 mW, t_{int} = 100 ms). Structures marked with arrows in the gray-scale images exhibit SERS activity.

satellite particles as well as their high colloidal stability are documented by the highly uniform UV/Vis extinction spectra recorded from seven different batches and from the comparison directly after the synthesis versus after four months (Figure S1), respectively.

Conjugates of the Au/Au core/satellite particles and the anti-hCG detection Ab were employed for the detection of the pregnancy hormone hCG in clinical serum samples from pregnant women (Scheme 1). The anti-hCG capture Ab at the TL and the control Ab at the CL were already immobilized on the nitrocellulose membrane of the commercially available hCG LFA. Figure 3a shows photographs of the LFA test strips in the presence of different hCG levels in the clinical samples. A concentration of at least 6.6 mIU mL^{-1} can be detected with the naked eye because of the blue-colored TL. This limit of detection (LOD) is approximately fourfold lower than the manufacturer's LOD of 25 mIU mL^{-1}. Figure 3b shows SEM images of the TL from a positive test (1679 mIU mL^{-1} hCG) and a negative control (no hCG) together with the corresponding Raman spectra: Only in the positive case several SERS nanotags bound to the nitrocellulose membrane can be detected. Figure 3c displays the concentration-dependent integrated Raman intensity of the dominant marker band at about 1064 cm^{-1} (see also Figure S3) as a function of the hCG concentration in the clinical samples. The corresponding Raman intensity at the TL is correlated to the number of SERS nanotags: High Raman intensities are observable for high hCG levels while no Raman signal is detectable for the negative control with no hCG. At high hCG levels (> 500 mIU mL^{-1}), saturation is observed, while at low hCG levels, a linear SERS response occurs. The SERS spectra of the strips with a hCG level of 0.8 mIU mL^{-1} and the negative control (0 mIU mL^{-1} hCG) are comparable. Thus, the LOD for the presented SERS-based detection is 1.6 mIU mL^{-1} (Figure 3c). This is 15 times lower compared to the LOD specified from the manufacturer of the commercially available LFA (25 mIU mL^{-1}). Overall, the SERS response curve in Figure 3c resembles the expected binding behavior for an LFA (for a comparison of the test performance of the Au/Au core/satellite conjugates and commercially available Au conjugates, see Figure S2).

The readout time for a SERS-LFA is a key parameter in POCT. A direct and fair comparison of previous SERS-LFAs with this work requires that the area of the entire TL is taken

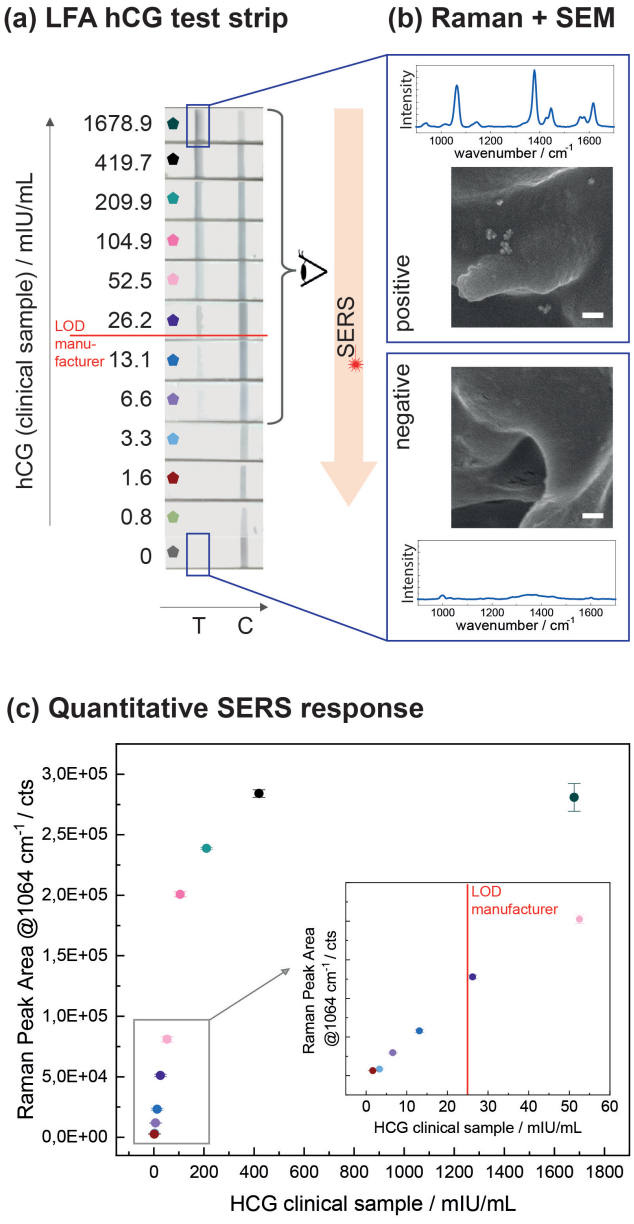

Figure 3. Concentration-dependent SERS-LFA of clinical serum samples from pregnant women. The SERS-labeled anti-hCG detection Ab was added to the NC membrane of the pregnancy test. a) Photographs of the test strips. b) SEM images (scale bar: 250 nm) of the TL from a positive test and a negative control together with the corresponding Raman spectra. c) Quantitative SERS response as a function of hCG concentration (λ_{ex} = 785 nm, laser power ca. 120 mW, 50 scans, t_{int} = 5 s). The LOD by SERS is 1.6 mIU mL^{-1}.

into account. Obviously, the readout time is reduced by several orders of magnitude when only a small portion of the entire TL with spatial undersampling is covered (for details regarding extrapolated acquisition times for full coverage of the TL without spatial undersampling, see the Supporting Information). In the present work, we covered the entire TL with dimensions of 4 mm × 0.8 mm in only 5 s without any undersampling. This is important for very low LODs as the Raman signal from the maximum possible number of SERS nanotags is recorded as well as for reproducibility.

In addition to hCG we also achieved the SERS-based detection of the two cytokines IL-6 and IL-8 as important markers of inflammation in humans and animals in a 2-plex assay (see Figures S4 and S5). Generally, the high sensitivity of the SERS-LFA technology (Figure 3c) is required for the early detection of analytes at very low concentrations. We envision that SERS-based POCT may become a transformative technology with the same sensitivity and reliability as current off-site laboratory diagnostics.

In summary, we have developed a portable SERS-LFA reader for fast test results within a few seconds, which is several orders of magnitude faster than previous readout schemes based on Raman microscopy with point illumination. Time is a highly critical and important parameter, for example, in clinical settings where patients with acute life-threatening symptoms need adequate treatment as fast as possible. The presented compact and affordable Raman instrumentation with line illumination through a custom-designed optical fiber probe in combination with ultrabright SERS nanotags paves the way towards making the powerful SERS technology available for real-world applications outside academic laboratories. Future instrumental improvements should consider further miniaturization and automation including software, while further applications should investigate the possibility of absolute quantification as well as the multiplexing potential for the simultaneous detection of multiple analytes (see Figure S6 for a SERS-based 5-plex on the same TL).

Acknowledgements

Financial support from the German Research Foundation (DFG; WA 3369/1-1) is highly acknowledged. We thank Ludmilla Langolf for the synthesis of spherical gold cores, Elzbieta Stepula for improving the synthesis of SERS C/S NPs, and Jörg E. Wissler for performing the correlative Rayleigh/SERS imaging.

Conflict of interest

The authors declare no conflict of interest.

Keywords: hCG pregnancy test · lateral flow assay · point-of-care testing · portable SERS reader · Raman spectroscopy

How to cite: *Angew. Chem. Int. Ed.* **2019**, *58*, 442 – 446
Angew. Chem. **2019**, *131*, 442 – 455

[1] a) R. C. Wong, H. Y. Tse et al., *Lateral Flow Immunoassay* (Eds.: R. C. Wong, H. Y. Tse), Springer, New York, **2009**; b) E. B. Bahadır, M. K. Sezgintürk, *TrAC Trends Anal. Chem.* **2016**, *82*, 286 – 306; c) G. A. Posthuma-Trumpie, J. Korf, A. van Amerongen, *Anal. Bioanal. Chem.* **2009**, *393*, 569 – 582; d) M. Sajid, A.-N. Kawde, M. Daud, *J. Saudi Chem. Soc.* **2015**, *19*, 689 – 705.

[2] a) *Surface Enhanced Raman Spectroscopy* (Ed.: S. Schlücker), Wiley-VCH, Weinheim, **2010**; b) S. Pahlow, A. März, B. Seise, K. Hartmann, I. Freitag, E. Kämmer, R. Böhme, V. Deckert, K. Weber, D. Cialla, J. Popp, *Eng. Life Sci.* **2012**, *12*, 131 – 143; c) R. A. Alvarez-Puebla, L. M. Liz-Marzán, *Small* **2010**, *6*, 604 – 610; d) Y. Wang, B. Yan, L. Chen, *Chem. Rev.* **2013**, *113*, 1391 – 1428; e) S. E. Bell, N. M. Sirimuthu, *Chem. Soc. Rev.* **2008**, *37*, 1012 – 1024; f) W. Xie, S. Schlücker, *Phys. Chem. Chem. Phys.* **2013**, *15*, 5329 – 5344; g) S. Schlücker, *Angew. Chem. Int. Ed.* **2014**, *53*, 4756 – 4795; *Angew. Chem.* **2014**, *126*, 4852 – 4894; h) Y. Wang, S. Schlücker, *Analyst* **2013**, *138*, 2224 – 2238; i) L. Fabris, *ChemNanoMat* **2016**, *2*, 249 – 258.

[3] a) J. Hwang, S. Lee, J. Choo, *Nanoscale* **2016**, *8*, 11418 – 11425; b) L. Blanco-Covián, V. Montes-García, A. Girard, M. T. Fernández-Abedul, J. Pérez-Juste, I. Pastoriza-Santos, K. Faulds, D. Graham, M. C. Blanco-López, *Nanoscale* **2017**, *9*, 2051 – 2058.

[4] a) S. Schlücker, *ChemPhysChem* **2009**, *10*, 1344 – 1354; b) M. Schütz, S. Schlücker, *J. Raman Spectrosc.* **2016**, *47*, 1012 – 1016; c) L. Rodriguez-Lorenzo, L. Fabris, R. A. Alvarez-Puebla, *Anal. Chim. Acta* **2012**, *745*, 10 – 23.

[5] a) W. Maneeprakorn, S. Bamrungsap, C. Apiwat, N. Wiriyachaiporn, *RSC Adv.* **2016**, *6*, 112079 – 112085; b) S. Choi, J. Hwang, S. Lee, D. W. Lim, H. Joo, J. Choo, *Sens. Actuators B* **2017**, *240*, 358 – 364; c) Y. Wang, M. Salehi, M. Schütz, S. Schlücker, *Chem. Commun.* **2014**, *50*, 2711 – 2714; d) R. Wang, K. Kim, N. Choi, X. Wang, J. Lee, J. H. Jeon, G.-e. Rhie, J. Choo, *Sens. Actuators B* **2018**, *270*, 72 – 79; e) Z. Rong, R. Xiao, S. Xing, G. Xiong, Z. Yu, L. Wang, X. Jia, K. Wang, Y. Cong, S. Wang, *Analyst* **2018**, *143*, 2115 – 2121; f) D. Zhang, L. Huang, B. Liu, H. Ni, L. Sun, E. Su, H. Chen, Z. Gu, X. Zhao, *Biosens. Bioelectron.* **2018**, *106*, 204 – 211; g) X. Jia, C. Wang, Z. Rong, J. Li, K. Wang, Z. Qie, R. Xiao, S. Wang, *RSC Adv.* **2018**, *8*, 21243 – 21251; h) T. Bai, M. Wang, M. Cao, J. Zhang, K. Zhang, P. Zhou, Z. Liu, Y. Liu, Z. Guo, X. Lu, *Anal. Bioanal. Chem.* **2018**, *410*, 2291 – 2303; i) X. Gao, P. Zheng, S. Kasani, S. Wu, F. Yang, S. Lewis, S. Nayeem, E. B. Engler-Chiurazzi, J. G. Wigginton, J. W. Simpkins, N. Wu, *Anal. Chem.* **2017**, *89*, 10104 – 10110; j) X. Fu, Y. Chu, K. Zhao, J. Li, A. Deng, *Microchim. Acta* **2017**, *184*, 1711 – 1719; k) Q. Shi, J. Huang, Y. Sun, R. Deng, M. Teng, Q. Li, Y. Yang, X. Hu, Z. Zhang, G. Zhang, *Microchim. Acta* **2018**, *185*, 84; l) X. Wang, N. Choi, Z. Cheng, J. Ko, L. Chen, J. Choo, *Anal. Chem.* **2017**, *89*, 1163 – 1169; m) H. B. Liu, X. J. Du, Y. X. Zang, P. Li, S. Wang, *J. Agric. Food Chem.* **2017**, *65*, 10290 – 10299; n) M. Sánchez-Purrà, M. Carré-Camps, H. de Puig, I. Bosch, L. Gehrke, K. Hamad-Schifferli, *ACS Infect. Dis.* **2017**, *3*, 767 – 776.

[6] S. Schlücker, M. D. Schaeberle, S. W. Huffman, I. W. Levin, *Anal. Chem.* **2003**, *75*, 4312 – 4318.

[7] M. Schütz, S. Schlücker, *Phys. Chem. Chem. Phys.* **2015**, *17*, 24356 – 24360.

[8] J. Wissler, M. Wehmeyer, S. Bäcker, S. Knauer, S. Schlücker, *Anal. Chem.* **2018**, *90*, 723 – 728.

Manuscript received: September 21, 2018
Accepted manuscript online: October 5, 2018
Version of record online: November 8, 2018

